Available online at www.sciencedirect.com

ScienceDirect

Materials Today: Proceedings 4 (2017) S128–S134

materialstoday: PROCEEDINGS

www.materialstoday.com/proceedings

NRW 2016

Lock-in Thermography for the Development of New Materials*

Peter W. Nolte[a]*, Timo Malvisalo[b], A. Charlotte Rimbach[b], Franziska Steudel[a], Bernd Ahrens[a,b], Stefan Schweizer[a,b]

[a]*Fraunhofer Application Center for Inorganic Phosphors, Branch Lab of Fraunhofer Institute for Microstructure of Materials and Systems IMWS, Lübecker Ring 2, 59494 Soest, Germany*

[b]*Department of Electrical Engineering, South Westphalia University of Applied Sciences, Lübecker Ring 2, 59494 Soest, Germany*

Abstract

Thermal management is one of the crucial concerns for mid- and high-power white light-emitting diodes (LEDs). Most of the currently available white LEDs on the market consist of a blue LED chip coated with a yellow phosphor-polymer composite. Besides the heat-induced degradation of the phosphor-polymer composite, the so-called thermal quenching, i.e. the decrease in light output upon increasing temperature, is also a pressing issue. Both result in an efficiency decrease and in a color change of the LED. In this work, a method to determine the thermal diffusivity and the thermal conductivity of phosphors is presented using lanthanide-doped glasses as test samples. In the quest for temperature-stable phosphors with a high thermal conductivity, such luminescent glasses might represent an attractive alternative. Thermal waves are introduced to the samples by periodical heating with a laser. Lock-in infrared thermography, a non-destructive method, is used to monitor even small changes in surface temperature. The phase delay of the thermal wave passing through the sample is analyzed at different lock-in frequencies and a mathematical fitting of the phase data then provides the coefficients required to determine the thermal diffusivity. Subsequently, the thermal conductivity is calculated from the thermal diffusivity, the mass density, and the specific heat capacity.

Selection and Peer-review under responsibility of 7th North Rhine-Westphalian Nano-Conference.

Keywords: lock-in thermography; thermal diffusivity; thermal conductivity; laser heating

* Corresponding author. Tel.: +49 2921 378 3555; fax: +49 2921 378 3600.

E-mail address: peter.nolte@imws.fraunhofer.de

Selection and Peer-review under responsibility of 7th North Rhine-Westphalian Nano-Conference.

1. Introduction

White light-emitting diodes (WLEDs) are currently revolutionizing the lighting market. These WLEDs are commonly comprised of a blue emitting LED chip and a yellow phosphor powder embedded in a polymer matrix on top [1]. The phosphor converts part of the blue light from the LED chip to longer wavelengths such that the combined spectra of the remaining blue radiation from the LED chip and the phosphor emission lead to a white color impression. During the light conversion process, heat is inevitably generated due to the energy difference between the primary blue and the generated longer wavelength photons [2, 3]. This heat is a substantial part of the overall losses of WLEDs adding up to the heat losses in the LED chip [4]. The phosphor-polymer composite, in particular the polymer, is prone to aging due to high temperatures and intense blue light radiation [5, 6].

Suitable candidates to replace the composite are luminescent glasses which possess high thermal and chemical stability. Luminescent glasses have attracted much attention in the last decades, in particular for applications such as lasers, optical fibers, and optical amplifiers. Borate glass is very versatile and a good host for luminescent lanthanide ions; it provides high optical transparency, good lanthanide ion solubility [7], and it can be cast in almost any shape or size. Nevertheless, in high-power applications such as laser-based remote phosphor concepts, the optical output power is limited by the temperature of the converter due to thermal quenching. For an efficient cooling of the phosphor, its thermal conductivity is an important parameter.

To analyze the thermal properties of lithium borate glasses optically-activated with different levels of europium ion concentration, thermal waves are introduced to the glass samples through periodical heating with a laser, which is synchronized to the image acquisition by an infrared camera. The phase delay between the triggering of the heat source and the thermal wave detected on the opposite side of the sample is then analyzed. A mathematical fitting of the frequency-dependent phase delay data provides the coefficients required to determine the thermal diffusivity of the material. Subsequently, the thermal conductivity of the material is calculated from the thermal diffusivity, the mass density, and the specific heat capacity [8–15].

2. Experimental details

2.1. Sample composition and preparation

The investigated borate glasses consist of the base components boron oxide (B_2O_3 from Alfa Aesar, 99.98 % purity) as network former and lithium oxide (Li_2O from Alfa Aesar, 99.5 % purity) as network modifier in the ratio of 2 to 1. The property modifier aluminum oxide (Al_2O_3 from Alfa Aesar, 99 % purity) is added for higher chemical stability and to reduce hygroscopicity. In addition, the glasses are doped with different amounts of europium oxide (Eu_2O_3 from Alfa Aesar, 99.99 % purity) for optical activation. The chemicals are mixed and afterwards melted in a platinum gold crucible (Pt/Au 95/5) at 1000 °C for approximately 3 h. For further details on the glass preparation, refer to [16, 17]. The exact compositions are summarized in Table 1.

Table 1. Nominal composition and thickness of the borate glass samples under study.

sample no.	composition in mol%				Eu^{3+} content	thickness
	B_2O_3	Li_2O	Al_2O_3	Eu_2O_3	in at.%	in mm
1	60.00	33.33	6.67	–	–	1.16
2	59.40	33.00	6.60	1.00	0.46	1.00
3	58.80	32.67	6.53	2.00	0.92	1.07
4	57.60	32.00	6.40	4.00	1.83	1.00

2.2. Measurement setups

The setup to measure the thermal diffusivity of the samples consists of an infrared (IR) camera (InfraTec ImageIR 8380S), a 980-nm laser diode (Thorlabs L980P100) with an optical output power of 100 mW for optical heating, a sample holder and a lock-in synchronization box, as shown in Fig. 1(a). The IR camera uses an indium antimonide (InSb) focal plane array (FPA) snapshot detector with a geometric resolution of 640 × 512 px²; the spectral range for detection is between 2.0 µm and 5.7 µm. For lock-in thermography measurements, the laser and the IR camera are connected to a control box synchronizing the image capturing and the laser pulses for different lock-in frequencies, f. The output of the laser is switched on and off by the synchronization box. Thus, the front side of the samples is periodically heated. Thermal waves are generated and travel through the sample. Subsequently, the phase delay of the thermal waves (relative to the laser triggering signal from the synchronization box) is monitored at the back side of the sample by recording the surface temperature with the thermographic system [13].

To exclude the effect of convection, the sample is placed in a closed vacuum chamber, depicted in Fig. 1(b). This chamber includes two glass windows: a sapphire glass that is transparent for IR radiation and a borosilicate glass transparent for the laser wavelength of 980 nm. For the measurements, the chamber is evacuated to pressures below 10 mbar.

The mass density, ρ, of the different glasses is measured by a density determination kit of an analytical balance (Mettler-Toledo XS105DU) based on the Archimedes principle. The specific heat capacity, c_p, is determined with a differential scanning calorimeter (Netzsch DSC 404 F1 Pegasus) according to DIN 51007 using sapphire as reference. The samples are cut into small pieces, ground in a mortar to a fine powder, and then filled in platinum rhodium crucibles (Pt/Rh 80/20). An empty crucible is used to measure the baseline. The temperature is increased with a heating rate of 20 K/min and the nitrogen flow is set to 20 ml/min during the measurements.

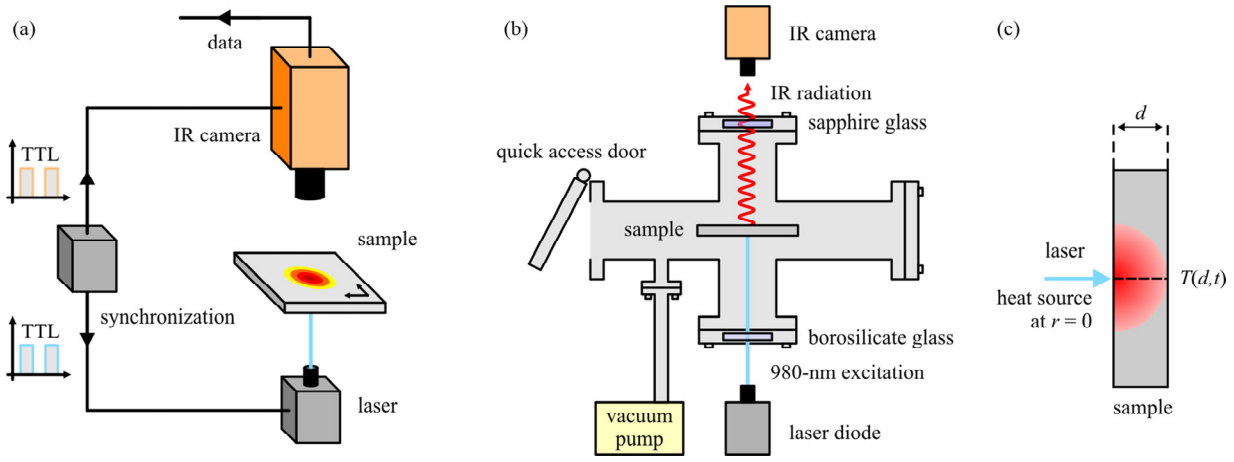

Fig. 1. (a) Principal lock-in thermography setup to measure the amplitude and phase information of thermal waves, (b) the vacuum setup used in the experiments, and (c) schematic view on the thermal wave propagation through the sample. The laser operates at a wavelength of 980 nm and has an optical output power of 100 mW. The sample surface is coated in black from both sides to increase optical absorption and thermal emission.

2.3. Evaluation of the phase values

In general, the temperature evolution, $T(r,t)$, at a time, t, and at a distance, r, of the sample in the experiment can be described by the heat equation

$$\frac{1}{\alpha}\frac{\mathrm{d}}{\mathrm{d}t}T(r,t)-\Delta T(r,t)=\frac{g}{k} \tag{1}$$

where k is the thermal conductivity, g the volumetric heat rate, and α the thermal diffusivity which is defined as:

$$\alpha=\frac{k}{\rho\cdot c_{\mathrm{p}}} \tag{2}$$

with ρ the mass density and c_{p} the specific heat capacity.

To calculate the temperature distribution in the experiment, the heat equation (1) needs to be solved with a harmonically oscillating point-like heat source at the front surface of the sample (r = 0) in spherical coordinates. Using the thermal diffusion length, $\mu=\sqrt{\alpha/(\pi\cdot f)}$, the angular frequency, $\omega=2\pi f$, and the sample thickness, d, the temperature at the back surface of the sample directly opposite to the laser, $T(d,t)$, as depicted in Fig. 1(c), can be described as [13]:

$$T(d,t)=\frac{A}{d}\cdot\exp\left(\frac{-d}{\mu}\right)\cdot\exp\left(\mathbf{i}\left(\omega t-\frac{d}{\mu}\right)\right). \tag{3}$$

The phase delay of the thermal wave, ϕ_{wave}, can be expressed as

$$\phi_{\mathrm{wave}}=\frac{d}{\mu}. \tag{4}$$

The total phase delay, ϕ, obtained from lock-in measurements, consists beside the phase of the heat wave, ϕ_{wave}, also of a system-depending phase delay, ϕ_{system}:

$$\phi=\phi_{\mathrm{system}}-\phi_{\mathrm{wave}}=\phi_{\mathrm{system}}-\frac{d}{\sqrt{\alpha/(\pi\cdot f)}}. \tag{5}$$

Given that the variable b is defined as

$$b=d\cdot\sqrt{\frac{\pi}{\alpha}}, \tag{6}$$

the phase delay, ϕ, of the thermal wave at the backside of the sample can consequently be expressed as follows:

$$\phi=\phi_{\mathrm{system}}-d\cdot\sqrt{\frac{\pi}{\alpha}}\cdot\sqrt{f}=\phi_{\mathrm{system}}-b\cdot\sqrt{f}. \tag{7}$$

For each sample, the lock-in frequency, f, is varied within a specific range. Subsequently, the corresponding phase delay, ϕ, is plotted versus the lock-in frequency, f. To determine the thermal diffusivity, α, the measured phase delay is analyzed on the basis of Eq. (7). The obtained fitting parameter, b, is then used to calculate the thermal diffusivity, α. Subsequently, the thermal conductivity, k, is calculated using Eq. (2).

3. Experimental results and discussion

3.1. Lock-in thermography parameters

To determine the thermal diffusivity, α, the amplitude and phase information of the generated thermal waves are measured. For each sample, a frequency range between 0.2 Hz and 1 Hz is used. Measurement period, required for the temperature, amplitude, and phase information to stabilize, is analyzed for each sample and an initial warm-up time of approximately 10 minutes is used to allow the samples to reach the thermal equilibrium prior to the measurements. The time between measurements at different frequencies is kept as short as possible to prevent cooling of the sample. After the initial warm-up, a temperature of 27 °C is observed at the area of heating for all samples at all lock-in frequencies. Figure 2(a) shows a thermographic image of an undoped lithium borate glass sample after 7 minutes of laser heating with a lock-in frequency of 0.2 Hz. Figure 2(b) shows the amplitude of the thermal waves at the position indicated in Fig. 2(a). A clear maximum of the amplitude is visible where the front side of the glass is hit by the laser. From this point outwards the amplitude of the thermal waves approaches zero Kelvin within a radius between 3 and 4 mm. For the analysis of the thermal diffusivity, the phase information as shown in Fig. 2(c) is directly recorded at the region of the maximum amplitude visible in Fig. 2(b).

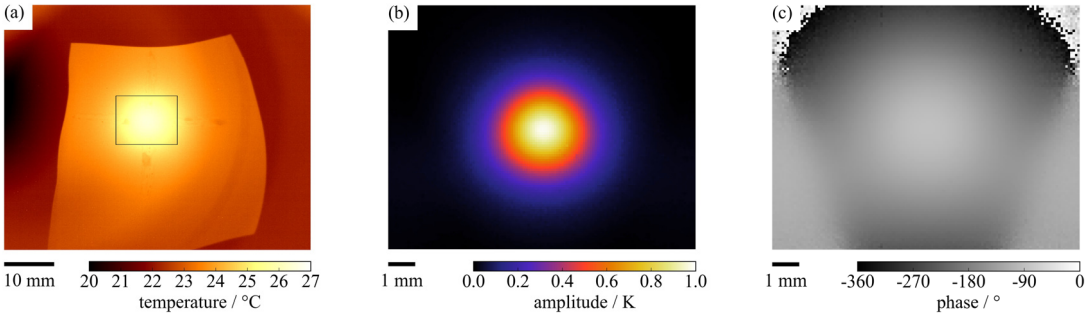

Fig. 2. As-recorded thermal image (a) of an undoped lithium borate glass (sample no. 1) under laser irradiation at a lock-in frequency of 0.2 Hz after 7 min of irradiation, together with close-up amplitude (b) and phase (c) images of the area indicated in Fig. 2(a).

3.2. Phase delay analysis and thermal diffusivity

Figure 3(a) shows the experimentally determined phase values (symbols) along with their corresponding fitting curves (solid lines) for all glass samples investigated. In Fig. 3(b), the phase data are thickness corrected and the frequency axis is scaled proportional to $f^{1/2}$. Thus, the slopes of the curves in Fig. 3(b) are proportional to the fitting parameter b as defined in Eq. (6). The resulting thermal parameters are summarized in Table 2. The europium ion concentration does not have a significant influence on the thermal conductivity of the lithium borate glass.

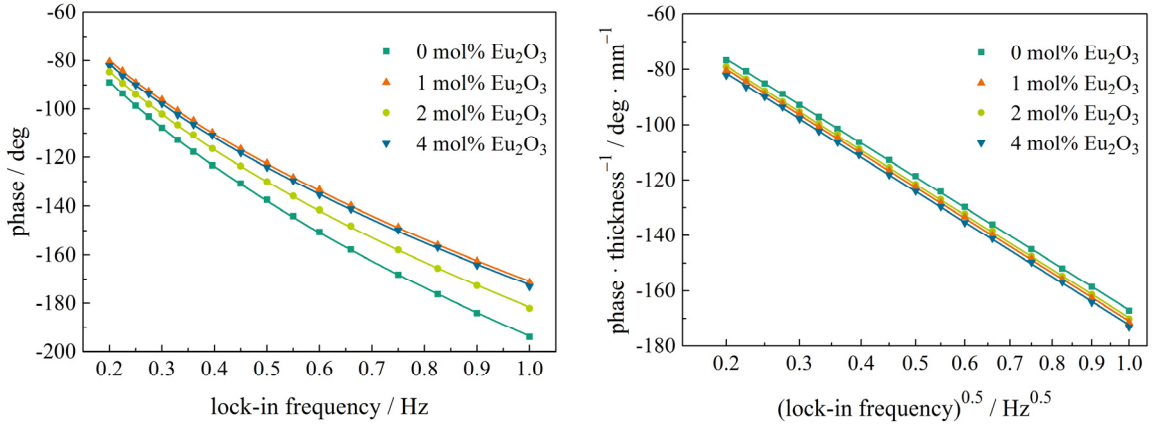

Fig. 3. (a) Experimental phase values (symbols) and the corresponding fitting curves (solid lines) together with (b) thickness-corrected phase data.

Table 2. Mass density, specific heat capacity, volumetric heat capacity, thermal diffusivity, and thermal conductivity for all samples investigated. All values are given at a temperature of 27 °C.

sample no.	Eu^{3+} content	mass density, ρ	specific heat capacity, c_p	volumetric heat capacity, $c_{p,V}$	thermal diffusivity, α	thermal conductivity, k
	in at.%	in g/cm^3	in J/(g · K)	in J/(cm^3 · K)	in 10^{-7} m^2/s	in W/(m · K)
1	–	2.26 ± 0.05	1.074 ± 0.046	2.43 ± 0.12	3.84 ± 0.07	0.93 ± 0.05
2	0.46	2.38 ± 0.05	1.019 ± 0.044	2.42 ± 0.12	3.81 ± 0.08	0.92 ± 0.05
3	0.92	2.48 ± 0.05	0.965 ± 0.041	2.39 ± 0.11	3.82 ± 0.07	0.91 ± 0.05
4	1.83	2.70 ± 0.05	0.898 ± 0.038	2.43 ± 0.11	3.81 ± 0.08	0.93 ± 0.05

3.3. Mass density and heat capacity

The results for the measurements of the mass density, ρ, and the specific heat capacity, c_p, are listed in Table 2. The mass density increases and the specific heat capacity decreases with increasing europium ion concentration. However, the volumetric heat capacity, $c_{p,V} = c_p \cdot \rho$, of the glasses is not affected by the change in europium ion concentration. A possible explanation for this observation might be that the europium ions are not part of the glass network and thus are not participating in the vibrations of the glass matrix (phonons). The volumetric heat capacity values are included in Table 2.

4. Conclusion

An approach based on lock-in thermography was used to measure the thermal diffusivity of lithium borate glasses with different europium ion concentrations. Lock-in thermography proved to be a suitable method to monitor even small changes in the thermal diffusivity values of the differently doped glasses. To determine the thermal conductivity of the investigated samples, their density and heat capacity were also measured. It was found that the europium ion concentration in the glasses has no significant influence on the thermal diffusivity or the volumetric heat capacity, and thus no effect on the thermal conductivity. As such it can be inferred that the europium ion concentration does not affect the thermal properties of the material. This behavior leads to the suggestion that europium ions do not participate in the vibrations of the glass matrix, possibly due to not being part of the glass network.

Acknowledgements

The authors wish to thank the "Ministerium für Innovation, Wissenschaft und Forschung des Landes Nordrhein-Westfalen" for its financial support to the Fraunhofer Application Center for Inorganic Phosphors in Soest as well as to the South Westphalia University of Applied Sciences within the FH STRUKTUR 2014 project "LED-2020". In addition, the authors would like to thank the German Federal Ministry for Education and Research (BMBF) for its support within the FHprofUnt 2014 project "LED-Glas" (project no. 03FH056PX4).

References

[1] T.Q. Khanh, P. Bodrogi, T.Q. Vinh, H. Winkler, LED Lighting: Technology and Perception, Wiley-VCH Verlag GmbH & Co. KGaA, 2014.
[2] X. Luo, X. Fu, F. Chen, H. Zheng, Phosphor self-heating in phosphor converted light emitting diode packaging, Int. J. Heat Mass Transf. 58 (2013) 276–281. doi:10.1016/j.ijheatmasstransfer.2012.11.056.
[3] M. Huang, L. Yang, Heat Generation by the Phosphor Layer of High-Power White LED Emitters, IEEE Photonics Technol. Lett. 25 (2013) 1317–1320. doi:10.1109/LPT.2013.2263375.
[4] X. Luo, R. Hu, Calculation of the phosphor heat generation in phosphor-converted light-emitting diodes, Int. J. Heat Mass Transf. 75 (2014) 213–217. doi:10.1016/j.ijheatmasstransfer.2014.03.067.
[5] E. Zanoni, M. Meneghini, N. Trivellin, M. Dal Lago, G. Meneghesso, GaN-based LEDs: State of the art and reliability-limiting mechanisms, in: 2014 15th Int. Conf. Therm. Mech. Multi-Phys. Simul. Exp. Microelectron. Microsyst. Eurosime, 2014: pp. 1–5. doi:10.1109/EuroSimE.2014.6813878.
[6] M. Buffolo, C. De Santi, M. Meneghini, D. Rigon, G. Meneghesso, E. Zanoni, Long-term degradation mechanisms of mid-power LEDs for lighting applications, Microelectron. Reliab. 55 (2015) 1754–1758. doi:10.1016/j.microrel.2015.06.098.
[7] D. Ehrt, Structure, properties and applications of borate glasses. Glass Technology Vol. 41 No. 6 (2000) 182-185.
[8] C. Boué, D. Fournier, Infrared thermography measurement of the thermal parameters (effusivity, diffusivity and conductivity) of materials, Quant. InfraRed Thermogr. J. 6 (2009) 175–188. doi:10.3166/qirt.6.175-188.
[9] C. Boué, S. Holé, Infrared thermography protocol for simple measurements of thermal diffusivity and conductivity, Infrared Phys. Technol. 55 (2012) 376–379. doi:10.1016/j.infrared.2012.02.002.
[10] F. Cernuschi, P.G. Bison, S. Marinetti, A. Figari, L. Lorenzoni, E. Grinzato, Comparison of thermal diffusivity measurement techniques, Quant. InfraRed Thermogr. J. (2002). doi:10.21611/qirt.2002.028.
[11] S. Chudzik, Measurement of thermal parameters of a heat insulating material using infrared thermography, Infrared Phys. Technol. 55 (2012) 73–83. doi:10.1016/j.infrared.2011.09.005.
[12] A.J. Angström, XVII. New method of determining the thermal conductibility of bodies, Philos. Mag. Ser. 4. 25 (1863) 130–142. doi:10.1080/14786446308643429.
[13] O. Breitenstein, W. Warta, M. Langenkamp, Lock-in Thermography, Springer Berlin Heidelberg, Berlin, Heidelberg, 2010. http://link.springer.com/10.1007/978-3-642-02417-7.
[14] X.P.V. Maldague, Nondestructive Evaluation of Materials by Infrared Thermography, Springer London, London, 1993. http://link.springer.com/10.1007/978-1-4471-1995-1.
[15] D. Wu, G. Busse, Lock-in thermography for nondestructive evaluation of materials, Rev. Générale Therm. 37 (1998) 693–703. doi:10.1016/S0035-3159(98)80047-0.
[16] F. Steudel, S. Loos, B. Ahrens, S. Schweizer, Multi-functionality of luminescent glasses for energy applications, Phys. Scr. 90 (2015) 094004. doi:10.1088/0031-8949/90/9/094004.
[17] F. Steudel, A.C. Rimbach, S. Loos, B. Ahrens, S. Schweizer, Effect of induced crystallization in rare-earth doped lithium borate glass, Radiat. Meas. 90 (2016) 274–278. doi:10.1016/j.radmeas.2015.12.046.